

MASTER

**Determination of fracture properties of cast steels  
(Project - JCU9S)**

by

S.I.Anderson and J.G.Loughran  
Department of Mechanical Engineering  
James Cook University of North Queensland

December 1998

18/12/98

## EXECUTIVE SUMMARY

Technology currently exists to estimate the structural durability of cracked sugar mill gears and mill roller shafts. Both SRDC projects JCU2S (Crack detection and durability assessment of low speed gears) and JCU6S (Finite element and durability modelling of roller shells and shafts) involve the application of linear elastic fracture mechanics to assess cracked components in Australian sugar factories. The benefits from these projects could not be fully realised due to the lack of fracture property data for Australian manufactured gear and shaft steels.

This project has utilised testing procedures according to ASTM standards to investigate fracture properties such as the Paris Law coefficient and exponent and the fracture toughness for candidate gear and mill roller steels. Four specimens from each material source were tested to provide preliminary fracture property data. These properties can now be used tentatively to assess the structural durability of cracked milling components manufactured from the same material as the candidate gear and shaft steels. A case study investigating the remaining life of a cracked mill roller using the experimental fracture properties is presented.

The experimental results reported have gone some way in completing our knowledge of the material characteristics of cast steels used in Australian sugar factories. Hence, a better understanding of how components will tolerate different operating conditions is now possible. Conceivable amendments to optimise condition monitoring are now possible using fracture mechanics theory and the appropriate material properties. However, it is recommended that further fracture based testing be undertaken to discover what effects operating conditions and manufacturing techniques have on the fracture properties of cast steels used in the extreme conditions imposed on milling equipment.

## CONTENTS

<b>1.0</b>	<b>Introduction</b>	1
<b>2.0</b>	<b>Research Plan</b>	2
2.1	KTH visit	2
2.2	Material sourcing	2
<b>3.0</b>	<b>Fracture mechanics theory</b>	4
3.1	Stress intensity	4
3.2	Crack propagation	10
<b>4.0</b>	<b>Experimental procedure (ASTM standards)</b>	14
4.1	Test method for measurement of fatigue crack growth rates	14
4.1.1	Introduction	14
4.1.2	Specimen size and apparatus	15
4.1.3	Terminology and test procedure	17
4.1.4	Interpretation of results	20
4.2	Test method for plane-strain fracture toughness of metallic materials	21
4.2.1	Introduction	21
4.2.2	Specimen size and apparatus	22
4.2.3	Terminology and test procedure	22
4.2.4	Interpretation of results	23
4.3	Test method for $J_{IC}$ , measure of fracture toughness	25
4.3.1	Introduction	25
4.3.2	Specimen size and apparatus	26
4.3.3	Terminology and test procedure	26
4.3.4	Interpretation of results	28
<b>5.0</b>	<b>Experimental results</b>	33
5.1	Results pertaining to candidate gear steel	33
5.2	Results pertaining to candidate roller shaft steel	42
<b>6.0</b>	<b>Case study - durability assessment of cracked mill roller shaft</b>	51
<b>7.0</b>	<b>Conclusions / recommendations</b>	59
	<b>References</b>	60
	<b>Appendices</b>	61
	Appendix 1 Mill roller geometry	61
	Appendix 2 Bending moment calculations	62

## 1.0 Introduction.

Over the past few years, SRDC has funded projects relating to durability analyses of cracked low speed gearing (JCU2S) and mill rollers (JCU6S). The benefits from these projects cannot be fully realised due to the lack of fracture property data for Australian manufactured gear and shaft steels. Data are available for similar US steels but there is no certainty that such properties pertain to Australian steels.

This project was initiated by Dr. Soren Ostlen, a senior lecturer in the Solid Mechanics Department at the Royal Institute of Technology (KTH) in Stockholm. Dr. Ostlen provided the opportunity for a JCU research officer to visit the KTH testing laboratory to observe the techniques and equipment requirements for producing fracture properties for engineering materials. KTH are recognised world leaders in fracture mechanics.

The successful completion of this project has provided fracture properties for use in previous projects JCU2S and JCU6S which involve life assessments for cracked large gears and roller shafts respectively. The determination of fracture properties for cast steels used in the sugar industry in combination with existing technology will aid mill engineers in the understanding of:

- What size cracks in roller shafts or large gear teeth can be tolerated under various loading conditions?
- How fast would a crack propagate until it reaches critical size?
- How often should cracked components be inspected?

Such knowledge could streamline condition monitoring procedures and reduce the occurrence of unexpected shutdowns due to roller shaft or large gear breakages.

The general aim of this project was to develop expertise in measuring fracture properties for cast steels. In addition, fracture properties of low speed gear steel and roller shaft steel were determined.

## **2.0 Research plan**

As stated in the SRDC project application, the objectives from this research were:

1. To gain expertise in measuring fracture mechanic properties for cast steels; and
2. To determine fracture properties of low speed gear steel and roller shaft steel.

These objectives were achieved by visiting KTH (Section 2.1) and participating in fracture testing of candidate gear steel sourced from an Australian sugar factory (Section 2.2). The testing facilities at JCU were found unsuitable to undertake fracture testing at the time of this project. Therefore, roller shaft steel was later sent to KTH for testing. JCU facilities will be upgraded to undertake such testing in early 1999.

### **2.1 KTH visit**

The author (Anderson) spent a total of four weeks at KTH. Three weeks were dedicated to observing the techniques and equipment requirements for producing fracture properties for engineering materials. The final week of the KTH visit was spent at a short course on 'Fatigue of materials' given by Prof. Subra Suresh from MIT.

Under the guidance of workshop manager Hans Oberg, the author participated in all aspects of fracture testing. Hans Oberg is an active member on the International standards committee (ISO). Specimen preparation, pre-cracking and final fracture testing procedures, and interpretation of results were undertaken on four specimens manufactured from the candidate gear material. An appreciation for equipment requirements and limitations was obtained. An improved understanding of fracture testing and associated operational guidelines was reinforced by witnessing several specimens which behaved uncharacteristically. Troubleshooting methods and acceptable alternative testing techniques were used to counter such phenomena.

Prof. Subra Suresh from MIT conducted a four day course based on the text, 'Fatigue of materials', (1996). The course covered such topics as: history of fatigue; cyclic damage and crack initiation in single crystals and commercial materials; total life and defect-tolerance approaches; basic fatigue fracture; numerical simulations of fatigue fracture; fatigue of polymers, ceramics, composites and laminates; and several case studies.

### **2.2 Material sourcing**

Sourcing suitable material for testing was achieved by visiting local sugar factories and foraging through their scrap yards. A failed final motion gear wheel was located at Macknade mill,

Ingham, as shown in Figure 2.1. Mill staff cut a 5 tooth section from the gear. This section was later machined at JCU's workshop into specimen blanks in preparation for the KTH visit.

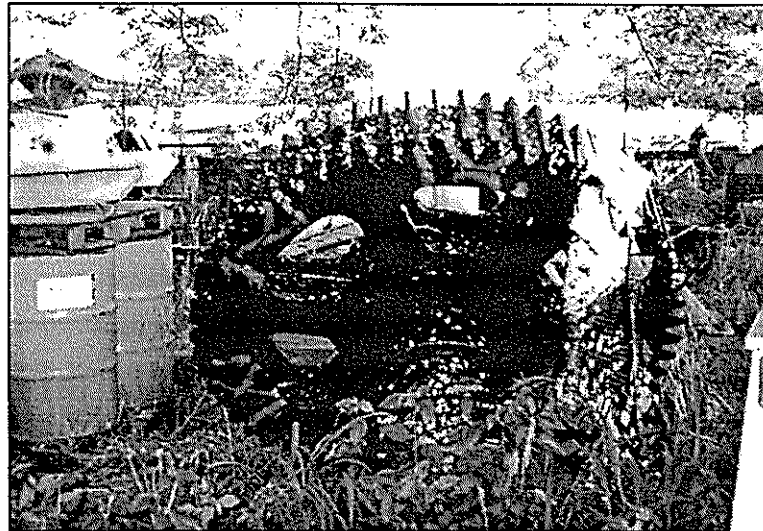


Figure 2.1 Gear wheel from which fracture specimens were sourced.

A failed top roller shaft was located at Pioneer mill, Brandon. The fractured drive-end stub was transported to Townsville Engineering Ltd. where a suitable sized section was removed as shown in Figure 2.2. This section was later machined at the JCU workshop into specimen blanks. Unfortunately, little information regarding the gear or roller shaft's manufacture was available. However, both components were manufactured in the early 1980s, typical of some equipment still operating in Australian factories.

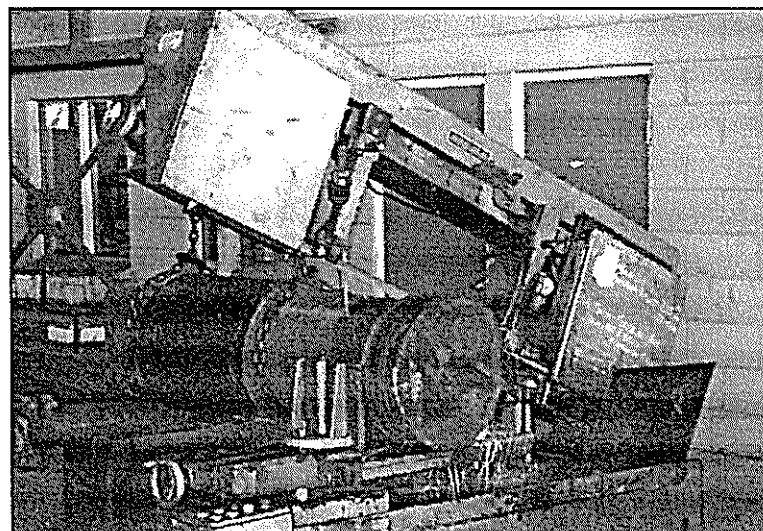


Figure 2.2 Roller shaft stub from which fracture specimens were sourced.

### 3.0 Fracture mechanics theory

This section covers basic fracture mechanics theory. The material properties required to assess the stability of cracks in mill components are discussed. The following is an abstract from Anderson and Loughran (1995).

#### 3.1 Stress intensity

The basic requirement of fracture mechanics theory is for assessment of the stability of cracks. A most significant advance has been the introduction of the 'Stress Intensity Factor' as a single parameter for categorising the onset of crack propagation. The direct relationship between the stress intensity factor ( $K$ ) and a material's toughness makes this approach attractive. However, the use of the stress intensity factor in investigating crack stability requires an accurate knowledge of the stress field in the vicinity of the crack tip. Analytical solutions exist for a wide range of simple cases, but recent improvements in numerical techniques such as finite element and boundary integral methods have made the determination of the stress and displacement fields for complex geometries and loading possible.

Life prediction for a cracked component can be determined through laboratory testing under simulated service conditions of geometry, loading and environment, or through the application of numerical methods adopting fracture mechanic's theory. Laboratory testing is expensive and time consuming as time-dependent corrosion effects prohibit test acceleration. However, computer based techniques can perform life predictions with similar accuracy to laboratory testing in a fraction of the time and cost. It would be impractical to physically test large components (eg. low speed mill gears or mill rollers) and difficult to simulate operational loading. However, computer based analysis techniques utilising material properties obtained from laboratory tests can be used to assess cracked components.

Under repeated loads above a certain level, a crack in a structure will grow in time (Broek, 1974). The larger the crack, the higher the stress concentration at the crack tip. Hence, the crack propagation rate should increase with time (Figure 3.1). The presence of a crack reduces the strength of the structure. The residual (remaining) strength decreases progressively as the crack size increases (Figure 3.2) and may decrease to a level where the structure would fail from an unexpected high service load. If such a load was not experienced, the crack would continue to grow whilst reducing the residual strength until it became so low that failure (fracture) would occur under normal service loading. In general, design engineers should account for the possibility of fatigue in structures. To ensure safety, a prediction of how fast cracks propagate (ie. how fast the residual strength decreases) needs to be made. Such predictions are possible through the application of fracture mechanics theory.

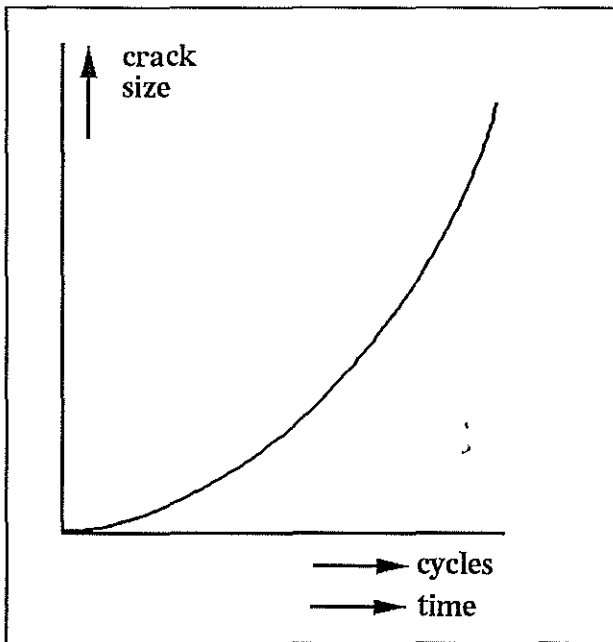


Figure 3.1 Crack growth curve.  
(after Broek, 1974).

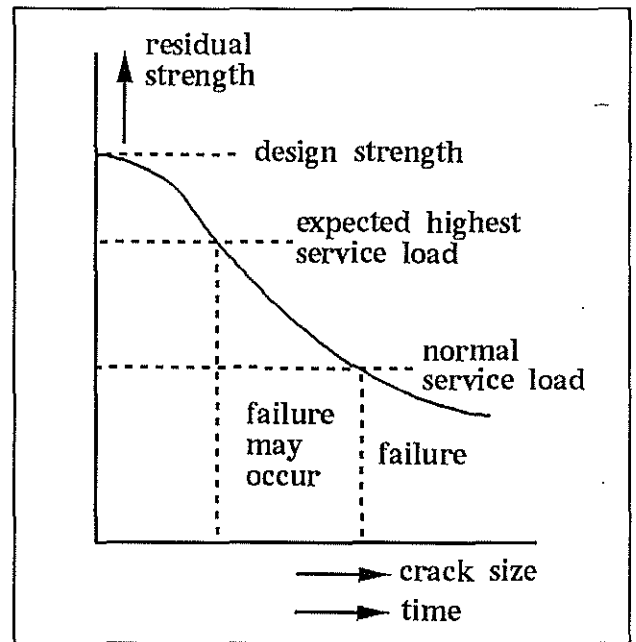


Figure 3.2 Residual strength curve.  
(after Broek, 1974).

A crack in a solid can be stressed in one or a combination of three different modes as seen in Figure 3.3. From a practical viewpoint, most common of these modes is the opening mode 'Mode I' (Broek, 1974).

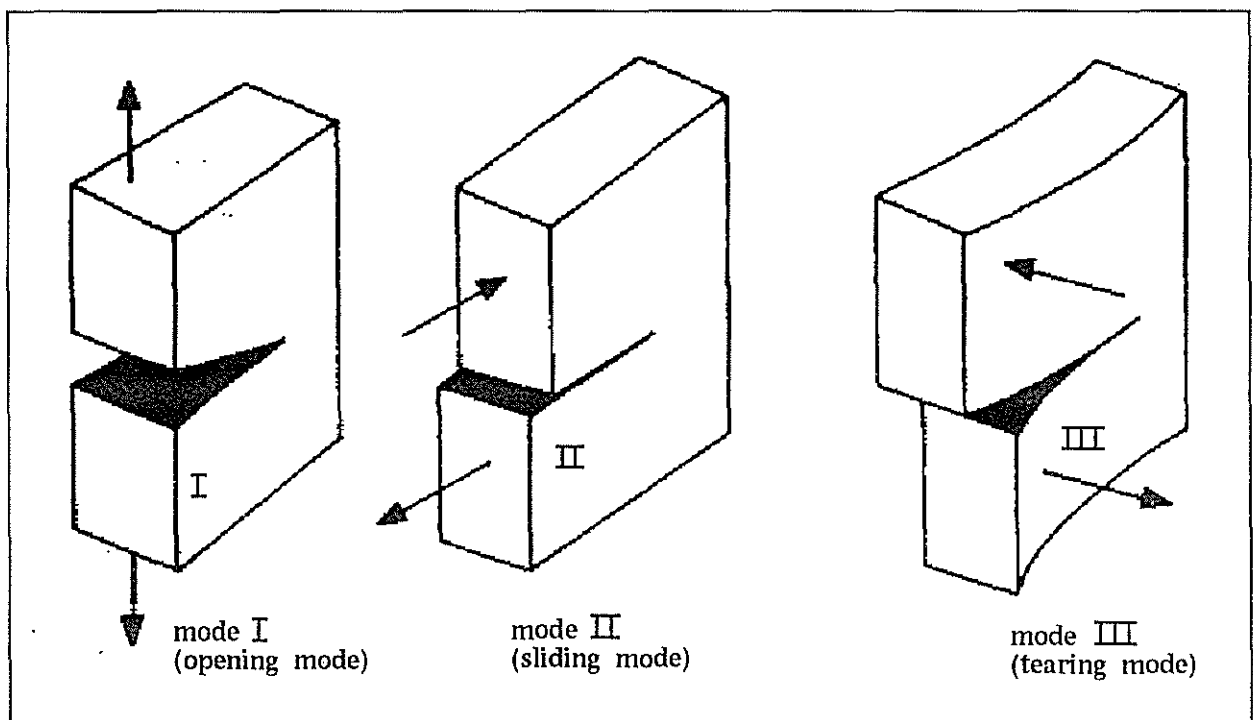


Figure 3.3 The three modes of loading (after Broek, 1974).

The elastic stress field ( $\sigma_{ij}$ , remote from the crack tip (position  $r, \theta$ )) of a 'through the thickness' crack in an arbitrary body experiencing a mode I loading (Figure 3.4) can be expressed as:

$$\sigma_{ij} = \frac{K_I}{\sqrt{2\pi r}} f_{ij}(\theta) \quad (3.1)$$

where  $f_{ij}(\theta)$  are known functions of  $\theta$ , and  $K_I$  is the stress intensity factor for mode I loading: Similar solutions are obtained for the other modes but with differing  $\theta$  functions.

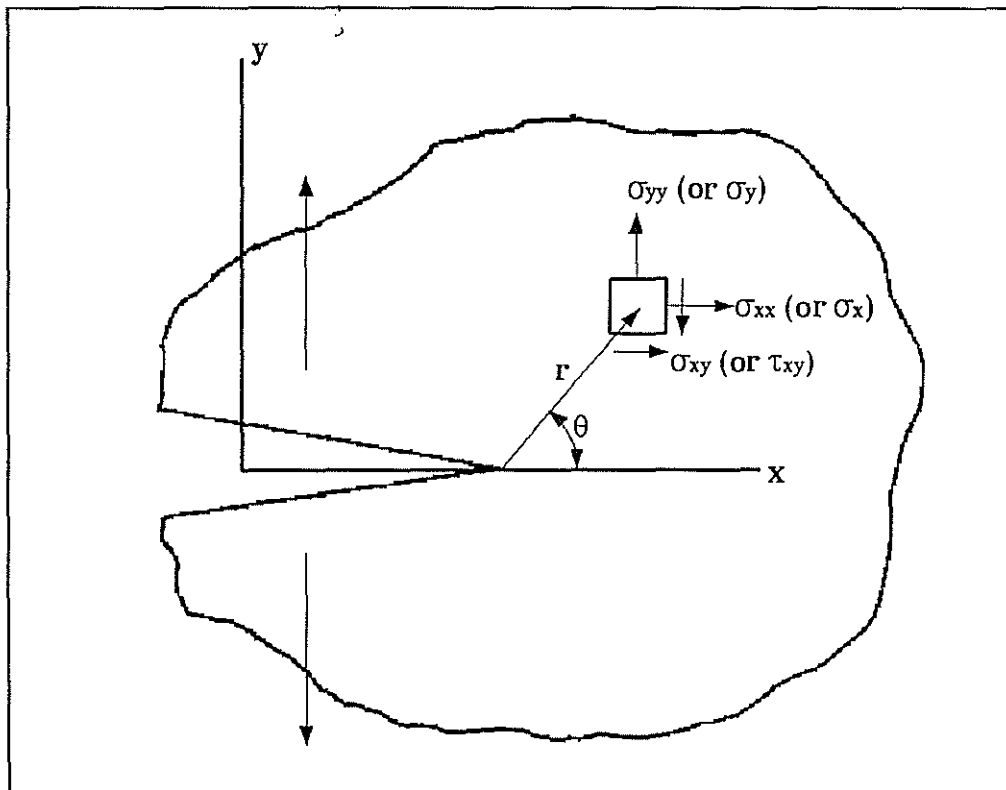


Figure 3.4 Crack in arbitrary body. (after Broek, 1974)

Combining the situation of an infinite plate under constant load or stress  $\sigma$  (Figure 3.5) with a central crack of length  $2a$  and applying equation 3.1 gives:

$$K_I = \beta\sigma\sqrt{a} \quad (3.2)$$

If, however, the width of the plate shown in Figure 3.5 is finite (of width  $W$ ), the crack tip stresses would increase from the case of the infinite plate. This suggests that  $K_I$  must increase with a decrease in  $W$ . Therefore, equation 3.2 should be modified to include a function of crack length divided by the width  $W$  for the case of the finite plate. Usually the stress intensity factors are expressed in relation to the stress intensity of the infinite plate mentioned previously, and therefore equation 3.2 becomes:

$$K_I = \beta\left(\frac{a}{L}\right)\sigma\sqrt{\pi a} \quad (3.3)$$

where  $L$  is a generalised size parameter and  $\beta\left(\frac{a}{L}\right)$  is a geometry function. The entire crack tip stress field can be described once the function  $\beta\left(\frac{a}{L}\right)$  is known. The fact that the net section stress increases with decreasing  $W$  is accounted for in  $\beta$ .

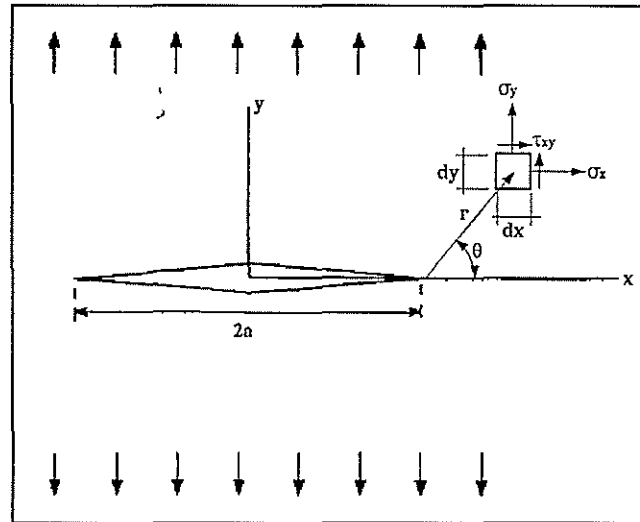


Figure 3.5 Crack in an infinite plate. (after Broek, 1974).

Geometry functions are generally written as high order polynomials such as:

$$\beta = C_1 + C_2\left(\frac{a}{L}\right) + C_3\left(\frac{a}{L}\right)^2 + C_4\left(\frac{a}{L}\right)^3 + C_5\left(\frac{a}{L}\right)^4 \dots \quad (3.4)$$

For example, the pre-calculated geometry function for the situation shown in Figure 3.6 is

$$\beta = 1.99 - 0.41\left(\frac{a}{W}\right) + 18.7\left(\frac{a}{W}\right)^2 - 38.48\left(\frac{a}{W}\right)^3 + 53.85\left(\frac{a}{W}\right)^4$$

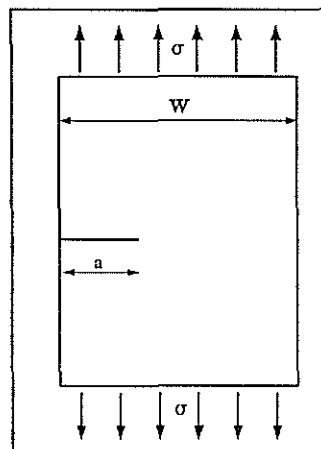


Figure 3.6 Crack in an infinite plate of width  $W$ . (after Broek, 1974).

Fundamental to fracture mechanics is that when the stress intensity of a crack reaches a certain value for that particular material, it will rapidly propagate causing component failure. Similarly, if the stress intensities for two cracked bodies (different physical size and crack size but of the same material) are equal then there is exact similitude. In other words, an equal stress intensity signifies similitude in stress at the crack tip.

The stress intensity at which a cracked component fails is known as the fracture toughness (or critical stress intensity) for that material. Although, the fracture toughness varies with temperature and environmental conditions, these are of second order importance compared to component thickness. The thickness of a component affects the fracture toughness value as the out-of-plane stresses (dependent on the thickness) determine the final size of the plastic zone at the crack tip (Figures 3.7 and 3.8).

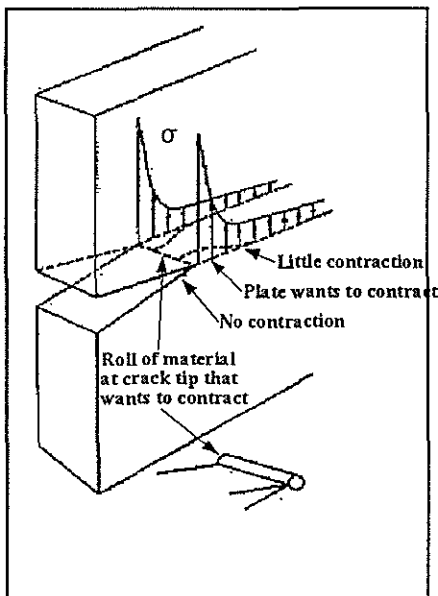


Figure 3.7 Contraction at crack tip.  
(after Broek, 1974)

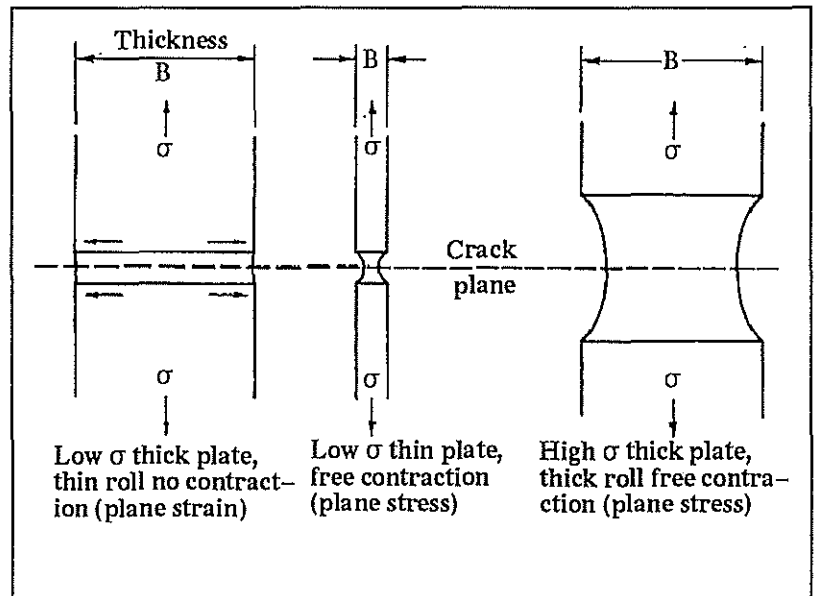


Figure 3.8 Schematic showing effect of thickness  
on stress state. (after Broek, 1974)

As displayed in Figure 3.7, the 'thin roll of material' (experiencing plastic deformation due to the high in-plane crack tip stresses mentioned previously) wants to contract due to Poisson's effect. The thickness of the component determines whether the surrounding material will allow contraction or not. If the thickness is sufficient to reduce the contraction of the plastic zone at the crack tip then stresses in the out of plane direction will be induced as shown in Figure 3.8. The presence of this additional stress at the crack tip affects the size of the plastic zone and stress field in front of the crack tip. Hence, the response of the crack changes depending on the thickness of the component. For cracks in thin section plates there is no restriction of the contraction of the crack tip plastic zone and this is referred to as 'plane stress'. In contrast where there is restriction of the crack tip plastic zone (eg. cracks in thick section plate), this is referred to as 'plane strain'.

The plane strain plastic zone is markedly smaller than the plane stress plastic zone. The effective yield stress in plane strain can be as high three times the uniaxial yield stress (Broek, 1974). The comparative stress distribution for plane stress and plane strain cases is shown in Figure 3.9. Note the relative size of the plastic zones ( $r_p$ ).

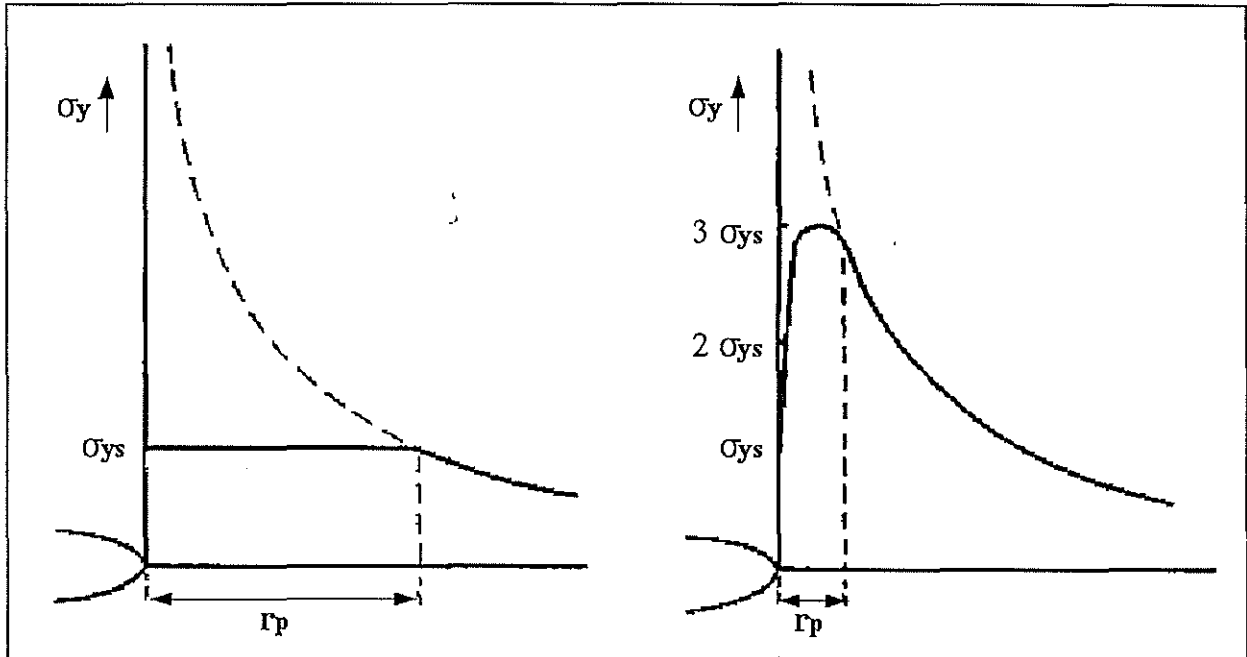


Figure 3.9 Typical stress distributions for plane stress (left) and plane strain (right).  
(after Broek, 1974)

For plane strain to exist along the majority of a crack tip front, the plate thickness must be adequately large. The thickness of a plate ( $B_s$ ) to ensure the condition of plane strain is :

$$B_s \geq 2.5 \left( \frac{K_I}{\sigma_{ys}} \right)^2 \quad (3.5)$$

where  $K_I$  is the applied stress intensity and  $\sigma_{ys}$  is the yield stress for the material. The fracture toughness is given the notation  $K_{IC}$  to represent mode I cracking. The dependency of  $K_{IC}$  and residual strength, upon thickness is shown in Figures 3.10 and 3.11. It can be seen that  $K_{IC}$  reaches a constant level after a certain thickness is obtained. The lower value for  $K_{IC}$  is generally used in design to ensure conservative results.

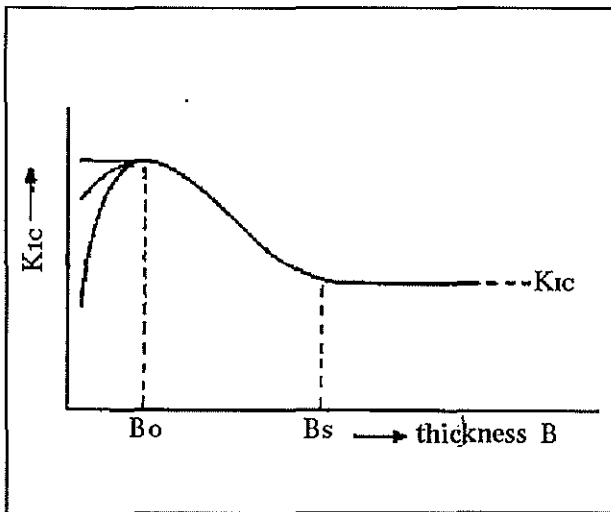


Figure 3.10  $K_{IC}$  vs. thickness.  
(after Broek, 1974).

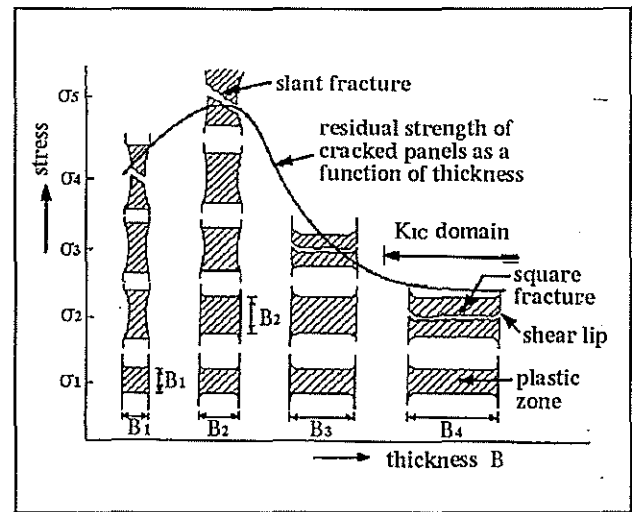


Figure 3.11 Residual strength vs. thickness.  
(after Broek, 1974).

Following Suresh (1991), if a crack length is increased by a small amount, the energy released per unit area of crack extension, ( $G$ ), is given by :

$$G_I = \left( \frac{\partial U}{B \partial a} \right) \tag{3.6}$$

where  $B$  is the thickness of the component and  $U$  is the potential energy. The stress intensity and the energy release rate have the following relationship (Suresh, 1991):

$$G_I = \frac{K_I^2}{E} \quad (\text{plane stress}) \tag{3.7}$$

or

$$G_I = \frac{K_I^2 (1 - \nu^2)}{E} \quad (\text{plane strain}) \tag{3.8}$$

or

$$G = G_I + G_{II} + G_{III} = \frac{(1 - \nu^2)(K_I^2 + K_{II}^2)}{E} + \frac{(1 + \nu)(K_{III}^2)}{E} \quad (\text{combined case}) \tag{3.9}$$

Finite element codes (eg. ABAQUS) calculate a J-Integral value (contour integral surrounding the crack tip) to determine the energy release rate  $G_I$  (J-Integral value =  $G_I$  ). This J-Integral calculation is a useful method for evaluating stress intensities.

### 3.2 Crack propagation

From equation 3.3, it's possible to predict the crack length for which a certain load would cause component failure if the fracture toughness was known and vice versa. The time it takes for a crack to reach a critical length for a known loading history is also of importance. Computer codes (PFATIGUE, NSOFT) can be used to assess the propagation of a crack in a structure. These

codes utilise the relationship between the increase in crack length per loading cycle and the change in the stress intensity per loading cycle. The basic form of this relationship as proposed by Paris in 1966 is based on experimental work carried out on pre-cracked material samples. The Paris Law (equation 3.10) in simplistic form, is obtained from the straight line section shown in Figure 3.12 which is representative of a steady state crack growth region.

$$\frac{da}{dN} = C(\Delta K)^m \quad (3.10)$$

where  $C$  and  $m$  (Paris Law coefficient and exponent) are proposed material constants and  $N$  is the number of repeated load cycles. Equation 3.10 is based on the case where the repeated loads are tensile (positive).

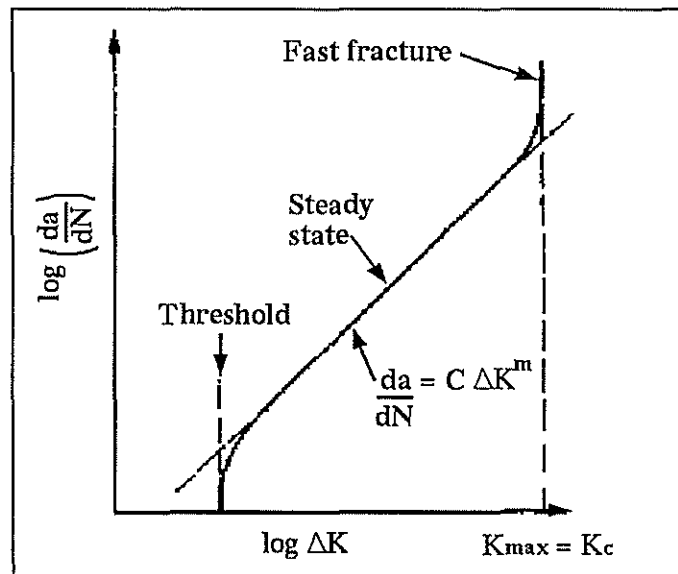


Figure 3.12 Common fatigue crack-growth rates.  
(after Ashby *et al*, 1982)

From Figure 3.12, it can be seen that the crack growth rate remains small ( $<0.1$  nm/cycle) until the change in stress intensity for a load cycle surpasses a threshold level. This threshold stress intensity level varies for different materials. Also of interest is the rapid increase in crack growth rate when the maximum stress intensity during a load cycle approaches or equals the fracture toughness value for a given material. At this point rapid failure occurs. Figure 3.13 illustrates the steady state growth of a crack and the increase in stress intensity for a cracked component under constant positive load cycling.

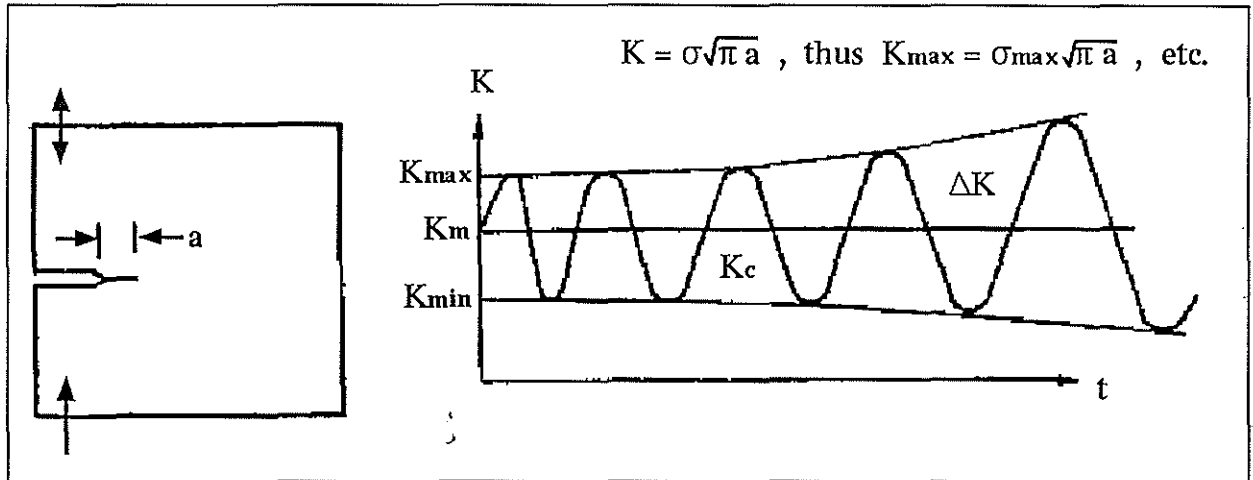


Figure 3.13 Example of fatigue crack growth.  
(after Ashby *et al.*, 1982)

There often exists a minimum crack size (short crack parameter) in components of a certain material and loading condition for which fracture mechanics theory is not applicable. According to Figure 3.12, the rate of propagation reduces significantly (assumed 0) when the operating stress intensity range ( $\Delta K$ ) falls below the material's threshold stress intensity level ( $K_{th}$ ). Equation 3.11 relates threshold stress intensity to a limiting fatigue crack size or short crack parameter ( $l_0$ ) as follows:

$$l_0 = \frac{1}{\pi} \left( \frac{\Delta K_{th}}{\Delta \sigma_0} \right)^2 \quad (3.11)$$

In Figure 3.13, the cyclic stress intensity increases with time as one would expect as the crack length, and hence the geometry function value increases. Therefore, for a cracked specimen undergoing repeated constant load cycles, the rate of crack growth continually increases until the crack reaches the critical crack length, at which point the maximum stress intensity equals the fracture toughness and rapid failure occurs.

A cycle by cycle fatigue crack propagation prediction code such as PFATIGUE calculates the crack extension for each load cycle in a load history and adds it to the current crack size. This process is repeated until the crack reaches the critical crack length. As previously mentioned, the driving force for crack propagation is the stress intensity range ( $\Delta K$ ). For each load cycle, the  $\Delta K$  calculated from the stress range, crack size and geometry function is known as the 'apparent or applied  $\Delta K$ '. To improve accuracy when using the Paris Law, this 'applied  $\Delta K$ ' is modified to obtain an 'effective  $\Delta K$ ' which accounts for the possible occurrence of crack closure, residual stresses, notch and environmental effects and negative loading ratios during each load cycle. Crack propagation life can therefore be predicted but only on a cycle by cycle basis. Smith (1991)

provides a simple method based on the Paris Law for estimating the propagation rate for a crack (equation 3.12) without the need for expensive computer codes.

$$N = \int_{a_i}^{a_f} \frac{1}{C(\Delta K)^m} da \quad (3.12)$$

where  $a_i$  = initial crack length  
 $a_f$  = final crack length

Rearranging equation 3.12, it becomes:

$$N = \frac{1}{C(\Delta\sigma\sqrt{\pi})^m} \int_{a_i}^{a_f} \frac{1}{\beta^m a^{m/2}} da \quad (3.13)$$

Assuming  $\beta$  does not change considerably (feasible for small crack extensions) and  $m$  does not equal 2, then equation 3.13 becomes:

$$N = \frac{1}{C(\beta\Delta\sigma\sqrt{\pi})^m} \left[ \frac{a_i^{1-m/2} - a_f^{1-m/2}}{m/2 - 1} \right] \quad (3.14)$$

A spreadsheet based on equation 3.14 can be used to approximate the number of cycles required for a crack to extend from  $a_i$  to  $a_f$  for several crack extension increments between the initial and final crack lengths and summing the resultant load cycle numbers. This method adopts the updated geometry function values for each crack extension increment and hence provides a more realistic cycle estimation.

## **4.0 Experimental procedure (ASTM standards)**

This section summaries the ASTM standards (1993 Annual book of ASTM standards - Section 3 - Metals Test Methods and Analytical Procedures) used in the determination of fracture properties for both large gears and mill roller shafts.

### **4.1 Test method for measurement of fatigue crack growth rates**

This section describes the procedure for determining the threshold stress intensity, Paris Law coefficient and exponent (Figure 3.12) whilst producing the pre-cracked specimen required for fracture toughness testing.

#### **4.1.1 Introduction**

This test method (E647-ASTM93) covers the determination of steady-state fatigue crack growth rates from near-threshold to fracture toughness controlled instability using compact tension (CT) specimens. Linear elastic theory is assumed, therefore specimen size must be sufficient to preclude buckling and remain predominantly elastic during testing.

Testing involves cyclic tensile loading of notched specimen which have been suitably precracked in fatigue. Measured crack length compared to elapsed load cycles establish the rate of crack growth. Fatigue crack growth rate expressed as a function of crack-tip stress intensity factor range,  $da/dN$  versus  $\Delta K$ , characterises a material's resistance to stable crack growth under cyclic loading. As  $da/dN$  versus  $\Delta K$  data are generally independent of planar geometry, they can be used in the design and evaluation of engineering structures (similitude concept).

In inert environments, fatigue crack growth rates are primarily a function of  $\Delta K$  and R (load ratio). However, several factors can affect  $da/dN$  versus  $\Delta K$  results and should be monitored during testing. Temperature and corrosive environments can significantly affect results. Specimen thickness effects can interact with other variables (eg. environment and heat treatment). If specimen thickness is inadequate, nominal yielding may occur before the stress intensity reaches the fracture toughness value. Residual stresses can influence crack growth behaviour as the effective stress state at the crack tip is not known with any certainty. Residual stresses usually cause irregular crack growth and excessive crack curvature. Small cracks (length comparable to microstructural dimension or crack tip plastic region) have been observed to exhibit greater growth rates than much longer cracks at similar loading levels. This phenomena has been attributed to environmental factors. Crack closure can have a dominant influence on crack growth rate behaviour at low stress ratios in the threshold regime due to the conditions in the wake of the crack

and prior loading history. Crack closure provides a mechanism whereby the effective stress intensity range near the crack tip differs from the applied values. This concept is important when interpreting crack growth rates since it implies a non-unique growth rate dependence in terms of  $\Delta K$  and load ratio.

In summary, this test method can serve the following purposes:

- establish the influence of crack growth on component life subject to cyclic loading if data are generated under representative conditions and combined with fracture toughness data;
- establish material selection criteria and inspection requirements for damage tolerant applications; and
- establish quantitatively, the effects of metallurgical, fabrication, environmental, and loading variables on fatigue crack growth.

#### 4.1.2 Specimen size and apparatus

Computer controlled testing was the preferred method chosen for all experimentation undertaken. The equipment required to perform this specialised testing is shown in Figure 4.1. Computer controlled testing requires a computer program based on the ASTM testing procedure to send digital load level, waveform and start / stop signals to the testing machine controller. Measured analogue data (crack mouth opening displacement from the clip gauge and applied loads from the testing equipment) is forwarded to the computer so as new updated control data can be returned to the testing machine controller. A general purpose interface bus board must be installed in the computer to deal with the analogue / digital conversions and to keep track of the load cycle count. Figure 4.2 details the fracture test configuration (testing machine, clevises and specimen).

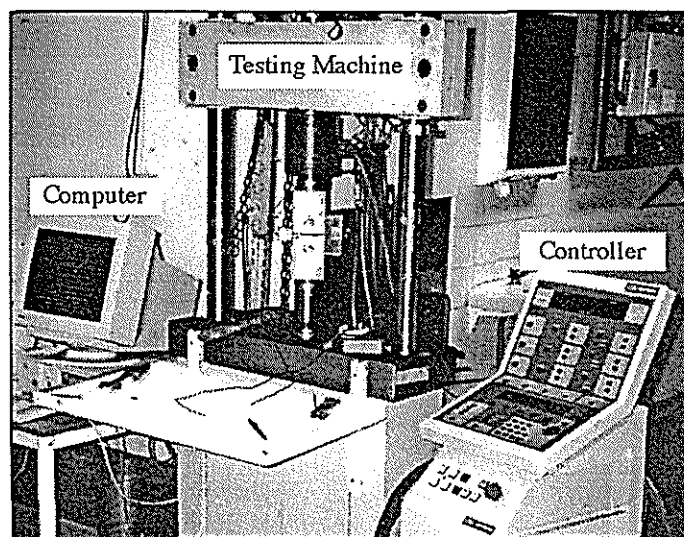


Figure 4.1 Equipment required for fracture testing.

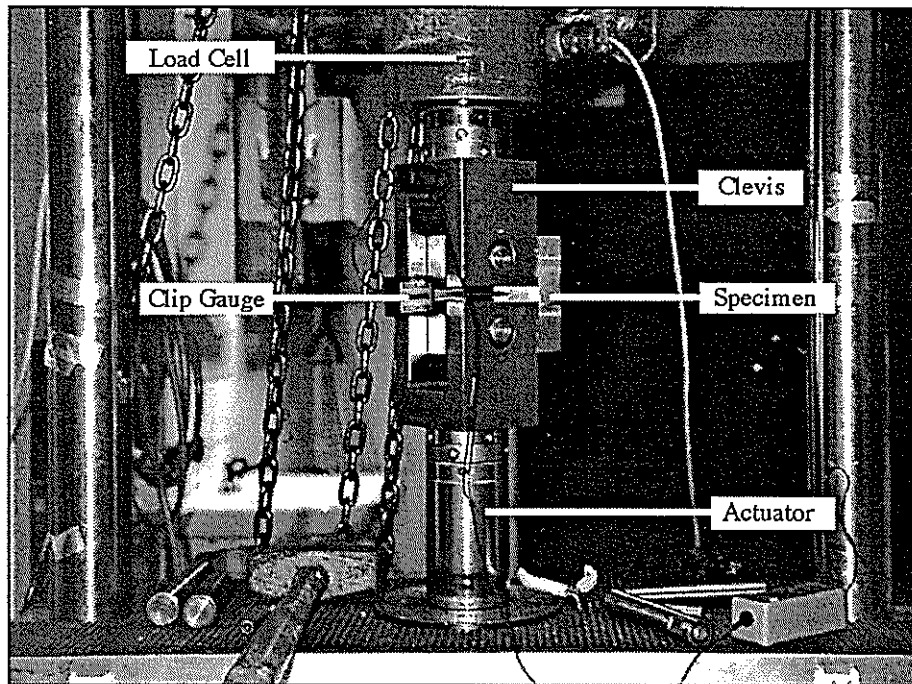


Figure 4.2 Fracture test configuration.

The CT specimen is not recommended for tension - compression testing, therefore all testing reported relates to cyclic tensile loading. Figure 4.3 illustrates the standard geometry requirements for a CT specimen. The clevis required to support the specimen is shown in Figure 4.4. Note that machining of the specimen and clevis surfaces should be parallel and perpendicular.

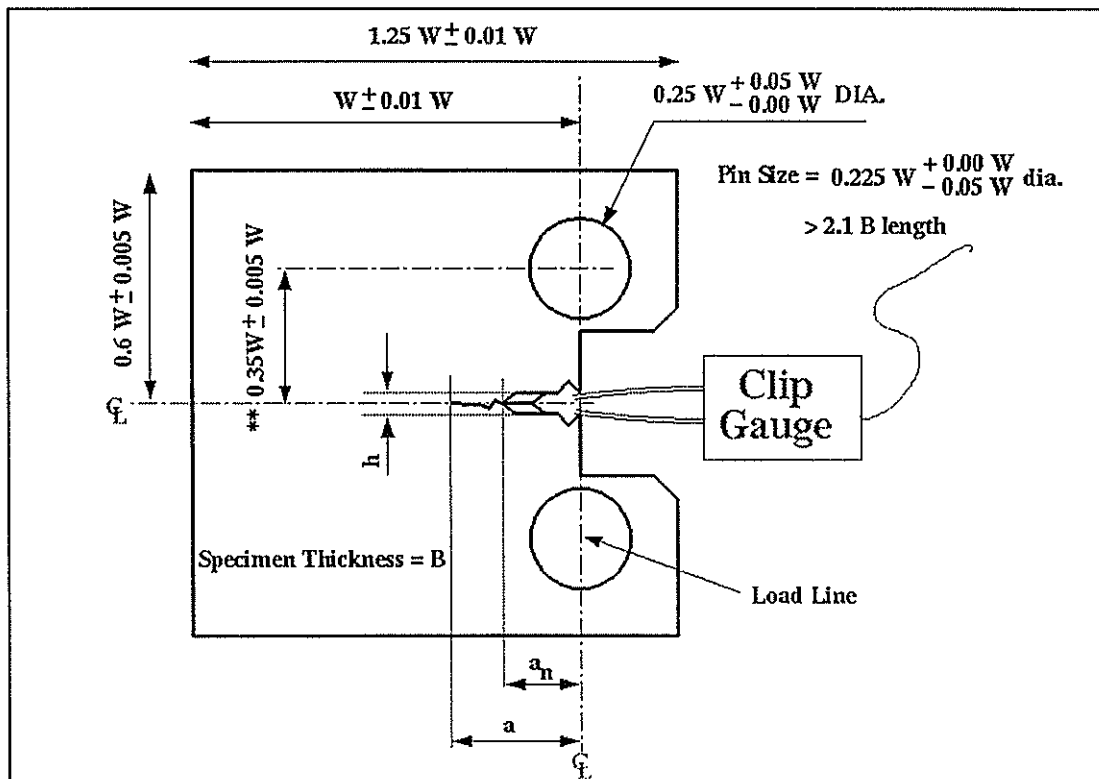


Figure 4.3 Standard CT specimen dimensions.

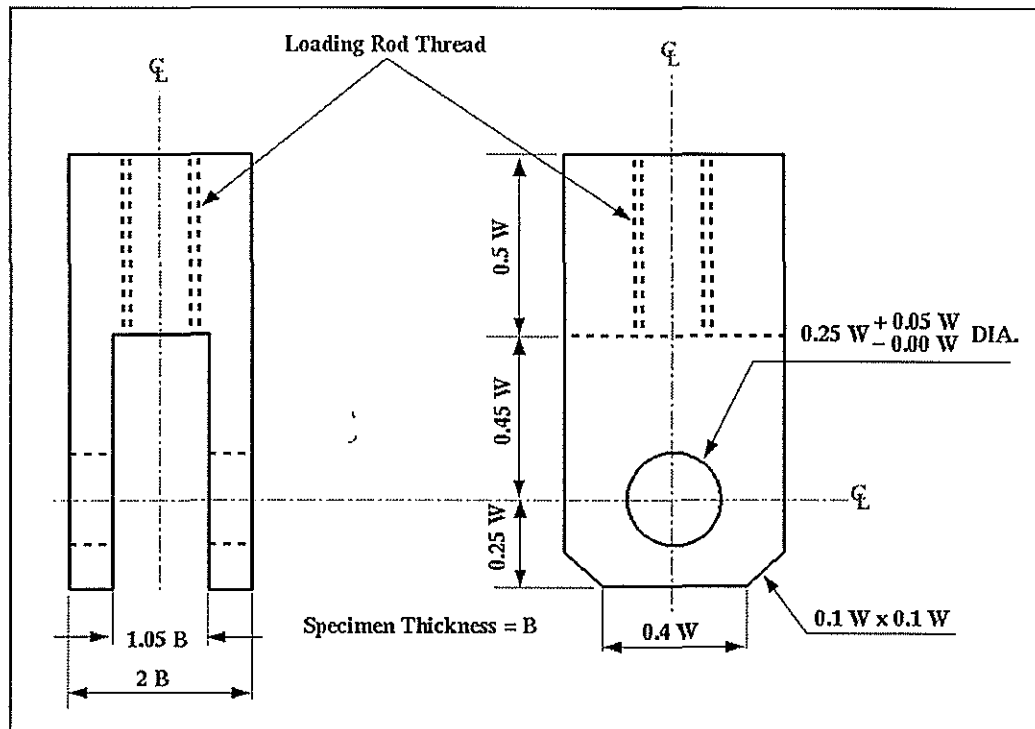


Figure 4.4 Standard clevis dimensions.

The pin-to-hole clearance (Figure 4.3) is designed to reduce non-linear load versus displacement behaviour. AISI 4340 steel is recommended for both clevis and pin construction as it should provide adequate strength and resistance to galling and fatigue. Some prior estimation of the fracture toughness, elastic modulus and yield strength for the specimen's material is required when calculating specimen size. For testing to be considered valid according to the standard, the following specimen dimensions must be adhered to (see Section 4.1.3 for definitions):

- $B \geq 2.5 \left( \frac{K_{Ic}}{\sigma_{fs}} \right)^2$  for compatibility with the plane strain fracture testing (Section 4.2);
- $\frac{W}{20} \leq B \leq \frac{W}{2}$  and  $W \geq 25 \text{ mm}$  ;
- $a_n \geq 0.2 W$  ; and
- $h \leq \frac{W}{16}$  .

#### 4.1.3 Terminology and test procedure

The following list is a set of definitions as adopted by the standard:

- crack size,  $a$ , measured from load line to crack front;
- fatigue crack growth rate,  $da/dN$ , crack extension per load cycle;
- load range,  $\Delta P$ , difference between maximum and minimum loads,  $P_{\max} - P_{\min}$ ;
- load ratio,  $R$ , ratio of minimum to maximum load,  $P_{\min} / P_{\max}$ ;
- stress intensity factor range,  $\Delta K$ , variation in stress intensity per load cycle,

$$\Delta K = K_{\max} - K_{\min} ;$$

$$\Delta K = (1-R) K_{\max} \text{ for } R \geq 0, \text{ and } \Delta K = K_{\max} \text{ for } R \leq 0 ;$$

- fatigue crack growth threshold,  $\Delta K_{th}$ , operational definition of  $\Delta K$  which corresponds to a fatigue crack growth rate of 0.1 nm / cycle;
- specimen width,  $W$ ;
- specimen thickness,  $B$ ;
- machined notch length,  $a_n$ ;
- chevron groove depth,  $h$ ;
- normalised K-gradient,  $C_n$ ; fractional rate of change of  $K$  with increasing crack length,  
 $C_n = dK / (K \cdot da)$  ;
- effective yield stress,  $\sigma_{fs}$ , yield stress value used in determination of specimen size,  
 $\sigma_{fs} = 0.2\%$  offset field stress ( $\sigma_{ys}$ ) for low strain hardening materials (ie.  $(\sigma_{ult} / \sigma_{fs}) \leq 1.3$ )  
or  $\sigma_{fs} = (\sigma_{ys} + \sigma_{ult}) / 2$  for high strain hardening materials (ie.  $(\sigma_{ult} / \sigma_{fs}) \geq 1.3$ ); and
- ultimate tensile strength,  $\sigma_{ult}$ .

During testing, the crack length ( $a$ ) must be measured frequently to determine stress intensity values and loading levels readjusted to adhere to the standard testing guidelines. To complete a test in a reasonable time frame, the compliance method for monitoring crack length was chosen over visual methods. Visual inspection of crack length is still used to ensure the compliance method is accurately determining the physical crack length. High speed digital data acquisition and processing systems are required to make use of the compliance method. Equation 4.1 gives the analytical relationship for compliance (reciprocal of load-displacement slope) and crack length measurement. Equation 4.1 assumes the clip gauge displacement was taken at the load line position as shown in Figure 4.3.

$$a = W (1.0002 - 4.0632 U_x + 11.242 U_x^2 - 106.04 U_x^3 + 464.33 U_x^4 - 650.68 U_x^5) \quad (4.1)$$

where  $U_x = \left\{ \left[ \frac{E v B}{P} \right]^{1/2} + 1 \right\}^{-1}$  ;

$$0.2 W \leq a \leq 0.975 W ;$$

$E$  = elastic modulus (can be adjusted to equalise physical and compliance crack length); and

$v/P$  = compliance = crack mouth opening displacement / applied load \*.

\* compliance value is usually taken from the upper linear portion of the load-displacement plot for each load cycle.

A variation of equation 4.1 (equation 4.2) is used in crack length calculations when the clip gauge reading is taken from the outer edge of the specimen (ie. 0.25  $W$  outside of load line).

$$a = W (1.0010 - 4.6695 U_x + 18.460 U_x^2 - 236.82 U_x^3 + 1214.9 U_x^4 - 2143.6 U_x^5) \quad (4.2)$$

From the crack length and applied load range,  $\Delta K$  can be calculated using equation 4.3.

$$\Delta K = \frac{\Delta P}{B \sqrt{W}} \frac{(2 + \alpha)}{(1 - \alpha)^{3/2}} (0.886 + 4.64 \alpha - 13.32 \alpha^2 + 14.72 \alpha^3 - 5.6 \alpha^4) \quad (4.3)$$

where  $\alpha = a/W$  and  $a/W \geq 0.2$ .

Prior to testing, the load cell and clip gauge should be calibrated to ensure measurements have an associated error of less than two per cent. The equipment should be capable of providing a symmetrical load distribution to the specimen notch. Fatigue precracking of the specimen is then required to produce a sharpened crack of adequate size and straightness. This crack should extend past the notch end by no less than  $0.1B$ ,  $h$  or  $1.0 \text{ mm}$ , whichever is greater. This precracking should be undertaken at the lowest possible stress intensity possible to avoid transient effects during initial crack growth measurements. The precrack length should be visually measured on both sides of the specimen to within  $0.1 \text{ mm}$  or  $0.002 W$ , whichever is greater. If these measurements differ by  $0.25 B$  then further testing would be considered invalid.

The objective of the crack growth rate testing is to develop a number of  $da/dN$  and associated  $\Delta K$  values from which a line of best fit can be made (Figure 3.12). Two standard test procedures exist. These are the K-increasing and K-decreasing test procedures. The K-increasing test procedure is best suited to crack growth rates above  $10^{-8} \text{ m/cycle}$  and the K-decreasing test procedure is best suited to crack growth rates below  $10^{-8} \text{ m/cycle}$ . It is considered good practice to conduct both K-increasing and K-decreasing tests such that overlapping regions of  $da/dN$  versus  $\Delta K$  data are obtained. Whichever method is chosen to commence testing, the applied  $K_{\max}$  should be greater than the final  $K_{\max}$  used in the precracking stage. This technique should avoid transient effects (retardation). When using the K-increasing procedure, incremental increases in the applied load should not exceed 10 per cent to minimise transient effects. Sufficient crack extension should be allowed following changes in load to enable steady state crack growth values.

The K-decreasing procedure is started by cycling at a  $K_{\max}$  ( $> K_{\max}$  from precracking) where subsequent load decreases (shedding) are introduced with crack growth. This technique is continued until test data are recorded for the lowest  $\Delta K$  or crack growth rate of interest is achieved. Load shedding during the K-decreasing test may be conducted as decreasing load steps at selected crack length intervals or continuously shed using a computer controlled technique. Either method should be gradual enough to allow at least 5  $da/dN$  versus  $\Delta K$  data points to be established every decade of crack growth rate. This can be achieved by limiting the normalised K-gradient,  $C$ , to be equal to or greater than  $-0.08 \text{ mm}^{-1}$ . It is recommended that the load ratio and normalised K-gradient remain constant during this test procedure. If incremental load shedding is employed, the drop in maximum load should be less than 10 per cent with an associated minimum crack extension of  $0.5 \text{ mm}$ . For a constant  $C$  test, equation 4.4 holds true.

$$\Delta K = \Delta K_0 \exp [C(a - a_0)] \quad (4.4)$$

where  $\Delta K_0$  and  $a_0$  are the respective values at the start of the test.

Crack length measurements should be taken at intervals to ensure even distribution with respect to  $\Delta K$ . The following intervals are recommended for a CT specimen:

- $\Delta a \leq 0.04 W$  for  $0.25 \leq a/W \leq 0.40$  ;
- $\Delta a \leq 0.02 W$  for  $0.45 \leq a/W \leq 0.60$  ; and
- $\Delta a \leq 0.01 W$  for  $0.60 \leq a/W$  .

Note, smaller  $\Delta a$  values as low as 0.25 mm may be required to obtain 5 da/dN versus  $\Delta K$  data points. Data should only be recorded when equation 4.5 holds true (specimen is predominantly elastic at all values of applied load).

$$W - a \geq \left( \frac{4}{\pi} \right) \left( \frac{K_{\max}}{\sigma_{ys}} \right)^2 \quad (4.5)$$

#### 4.1.4 Interpretation of results

The precision of da/dN versus  $\Delta K$  is a function of material variability and measurement errors concerning crack length and applied load. The standard states that there is no 'standard' value for da/dN versus  $\Delta K$  for any material. An extensive laboratory testing program showed that the reproducibility in da/dN within a laboratory to average  $\pm 27$  per cent and between laboratories,  $\pm 32$  per cent. All equations used are based on the assumption that the test specimen material is linear-elastic, isotropic and homogeneous. Residual stress and crack closure are not considered in the determination of the  $\Delta K$  values.

Upon completion of the fatigue cracking, the specimen is completely fractured (fracture toughness testing, Sections 4.2 and 4.3) so that the crack front (curvature and length) can be measured. The difference between the average through-thickness crack length and the corresponding crack length recorded using the compliance method is referred to as the crack curvature correction. If the crack curvature correction magnitude increases or decreases with crack length, a linear interpolation is used to correct intermediate data points. The test is considered invalid if the crack deviates more than  $20^\circ$  from the symmetry plane over a distance equal to  $0.1 W$ .

The rate of fatigue crack growth is determined from the crack length versus elapsed load cycle data (a versus N). The secant method (equation 4.6) is one technique for computing crack growth rates.

$$\frac{da}{dN} = (a_{i+1} - a_i) / (N_{i+1} - N_i) \quad (4.6)$$

The corresponding  $\Delta K$  value with the  $da/dN$  value is calculated using the average crack length for the interval. The crack length interval chosen should be large compared to the measurement error but small compared to the  $K$ -gradient of the test specimen. This crack growth rate determination shall not be made over any increment of crack extension which includes a load step.

A straight line (best-fit) can be plotted from a linear regression of  $\log da/dN$  versus  $\log \Delta K$  using a minimum of five data points of approximately equal spacing between growth rates  $10^{-9}$  and  $10^{-10}$  m/cycle. The resulting best-fit line equation can be used to determine the threshold stress intensity corresponding to a growth rate of  $10^{-10}$  m/cycle.

## 4.2 Test method for plane-strain fracture toughness of metallic materials

This section describes the procedure for determining the plane strain fracture toughness ( $K_{IC}$ , Figure 3.10) using fatigue cracked specimens.

### 4.2.1 Introduction

This test method (E399-ASTM93) covers the determination of the plane strain fracture toughness using fatigue cracked CT specimens having a thickness greater than 1.6 mm. As there is no assurance that a valid  $K_{IC}$  will be determined in a particular test, the standard also covers the determination of the specimen strength ratio  $R_S$ .

Testing involves an increasing tensile load being applied to a suitably precracked specimen. The measured load versus crack mouth opening displacement are recorded. The load corresponding to a two per cent apparent increment of crack extension is established by a specified deviation from the linear portion of the recorded data plot (Section 4.2.4).  $K_{IC}$  is calculated from this load by equations based on elastic stress analysis of CT specimens. The precracking procedure and specimen size determine the validity of the  $K_{IC}$  value.

The property  $K_{IC}$  characterises the resistance of a material to fracture in a neutral environment in the presence of a sharp crack under severe tensile constraint (triplane strain stress state at crack tip). The crack tip plastic region is small in comparison to the crack and specimen size.  $K_{IC}$  is considered the limiting value of fracture toughness. Note that the  $K_{IC}$  value determined using this test method is a function of testing speed and temperature. Therefore, the application of  $K_{IC}$  in design of a component needs to consider the difference that may exist between laboratory tests and field conditions. Similarly, fracture toughness of a material can depend on the orientation and direction of crack propagation in relation to anisotropy of the material.

In summary, this test method can serve the following purposes:

- establish the effects of metallurgical variables such as composition, heat treatment or fabrication on the fracture toughness;
- establish the suitability of a material for a specific application for which maximum flaw sizes are known with certainty; and
- establish a  $K_{IC}$  value in relation to a particular design for use in fracture control under known loading and environmental histories.

#### 4.2.2 Specimen size and apparatus

Testing apparatus required is identical to that described in Section 4.1.2. To reduce time and costs associated with all aspects of fracture testing, the CT specimens used in the determination of fatigue crack growth rates were used in this plane strain fracture toughness testing. The two respective standards were used to ensure that the precracking stage was appropriate for fracture toughness evaluation.

Calibration of all measuring equipment is required prior to testing. The crack mouth opening displacement (clip) gauges should have a linearity which corresponds to a maximum deviation of 0.0025 mm over the working range.

For a  $K_{IC}$  test to be considered valid, the following dimensions are required:

$$B \geq 2.5 \left( \frac{K_{IC}}{\sigma_{fs}} \right)^2 ;$$

$$2 \leq \frac{W}{B} \leq 4 \quad (W = 2B \text{ is most common ratio used}); \text{ and}$$

$$0.45 \leq \frac{a}{W} \leq 0.55.$$

A chevron notch is the recommended fatigue crack starter geometry for this test method.

#### 4.2.3 Terminology and test procedure

See Section 4.1.3 for parameter definitions.

The production of a satisfactory precrack is required before a valid plane strain fracture toughness test can commence. This precrack needs to extend past the notch by a minimum of 1.25 per cent of the width on both sides of the specimen. The precracking procedure used in this report consisted of the crack growth rate testing (Section 4.1). In addition to these guidelines, it is recommended that the final 2.5 per cent of the final crack length be produced using an applied  $K_{max}$

less than 60 percent of the expected  $K_{IC}$  value and the ratio between  $K_{max}$  and the elastic modulus not exceed  $0.00032m^{1/2}$ .

It is considered good practice to undertake at least three replicate tests for each material. The test procedure itself is straight forward. Upon completion of the precracking phase, the specimen is continually loaded at a rate which corresponds to an increase of stress intensity within the range, 0.55 to 2.75 MPa.m<sup>1/2</sup>/s. The test continues until the specimen can no longer sustain any further load increase. The specimen can then be pulled apart to expose the fracture surface for inspection. The load and crack mouth opening displacement are continually logged using computer based data acquisition or plotted using an autographic machine. Section 4.1 describes the method for recording applied load and crack mouth opening displacements using a computer and calculating crack lengths and associated stress intensities.

#### 4.2.4 Interpretation of results

The precision of a  $K_{IC}$  determination depends in part on the errors in the load, crack mouth opening displacement and specimen dimension measurements. The standard states that there is no 'standard' value for plane strain fracture toughness of any material.

To establish a value for  $K_{IC}$ , it is necessary to calculate a conditional result,  $K_Q$ , which involves an analysis of the test record (load versus crack mouth opening displacement plot). The procedure is as follows (see Figure 4.5 for description):

1. Draw a secant line through the origin of the test record with slope  $(P/v)_5 = 0.95(P/v)_0$ , where  $(P/v)_0$  is the slope of the tangent OA to the initial linear section of the record. The load  $P_Q$  (used to calculate  $K_{IC}$ ) can then be determined as follows:
  - if the load at every location on the record preceding  $P_5$  is less than  $P_5$ , then  $P_5$  is  $P_Q$ , else if there is a maximum load preceding  $P_5$  which is greater than  $P_5$ , then this maximum load is  $P_Q$ .
2. Calculate the ratio  $P_{ax}/P_Q$ , where  $P_{max}$  is the maximum load the specimen was able to sustain during testing. If  $P_{max}/P_Q$  does not exceed 1.10 then  $P_Q$  can be used to determine a  $K_{IC}$  value. If the ratio exceeds 1.10 then the test is considered invalid.
3. If both specimen thickness and crack length are greater than  $2.5 (K_Q/\sigma_{ys})^2$  then  $K_Q$  can be used to determine a  $K_{IC}$  value, otherwise the test is considered invalid.

A modified version of equation 4.3 can be used to calculate  $K_Q$  ( $K_{IC}$ ).

$$K_Q = \frac{P_Q}{B \sqrt{W}} \frac{(2 + \alpha)}{(1 - \alpha)^{3/2}} (0.886 + 4.64 \alpha - 13.32 \alpha^2 + 14.72 \alpha^3 - 5.6 \alpha^4) \quad (4.7)$$

where  $\alpha = a/W$ .

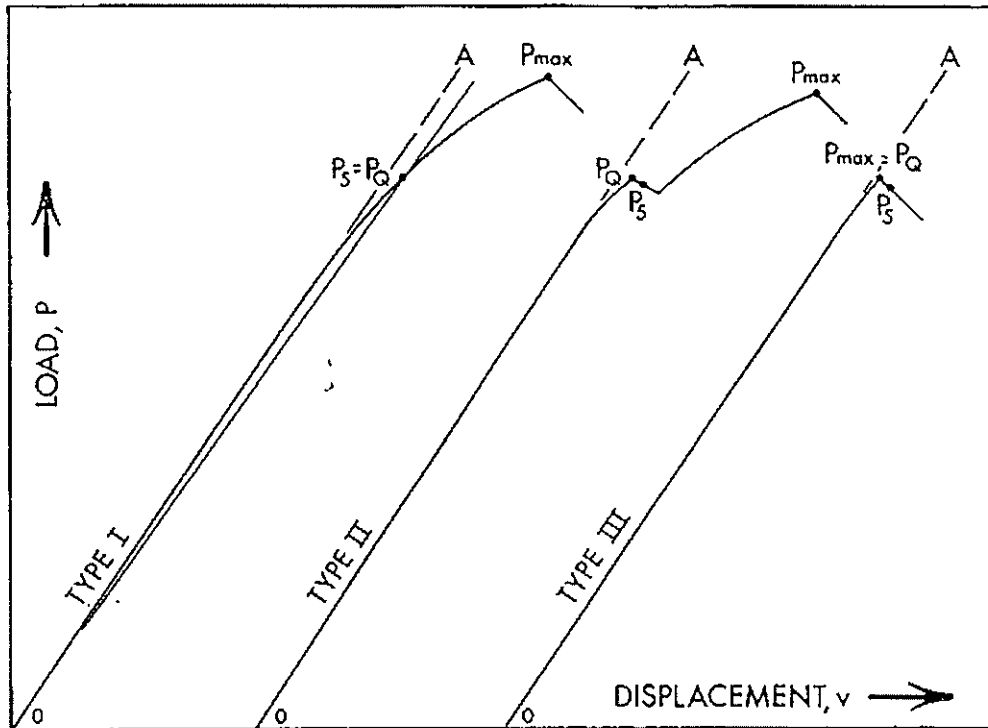


Figure 4.5 Principal types of load-displacement records.

The crack length should be visually measured at the completion of the test. Three measurements, one in the centre and one either side of the centre, half way to the unnotched sides are needed. If the difference between any two of these readings is greater than 10 per cent of the average crack length or the surface crack length measurements differ by more than 10 per cent from the average than the test is considered invalid. The central plane of the crack should not differ by more than  $10^\circ$  off symmetry or again the test is considered invalid. The appearance of the fracture surface (Figure 4.6) can add valuable supplementary information. The proportion of oblique fracture per unit thickness  $((B-f)/B)$  should be noted.

As in crack growth rate testing, the actual measured crack length should be compared to the compliance based crack length prediction. Any discrepancies can be accounted for by adjusting the value of  $E$  in equation 4.1 to correct the compliance measurements.  $E$  in this case may need to be altered to the effective elastic modulus  $E_M (= E/(1-\nu^2))$  where  $\nu$  equals Poissons ratio for the material. Linear interpolation can also be used to correct intermediate data points.

In this case where the test results render the  $K_{IC}$  value invalid, the strength ratio,  $R_S$ , can be calculated as in equation 4.8. This dimensionless value is a function of the maximum test load, specimen dimensions and the yield strength of the material.  $R_S$  can be compared with different materials and preparations, but of the same specimen geometry, when selecting a material for a particular design.

$$R_s = \frac{2P_{\max} (2W + a)}{B (W - a)^2 \sigma_{ys}} \quad (4.8)$$

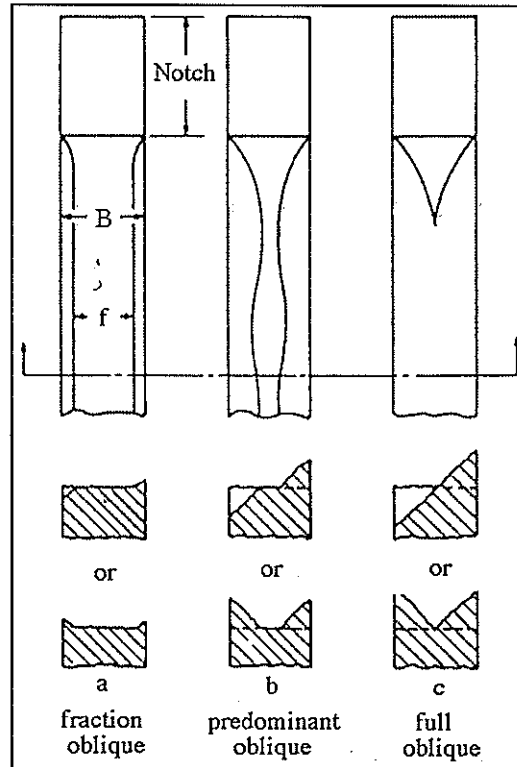


Figure 4.6 Common types of fracture appearance.

### 4.3 Test method for $J_{IC}$ , measure of fracture toughness

This section describes the procedure for determining  $J_{IC}$ , which can be used as an engineering estimate of fracture toughness near the initiation of slow stable crack growth.

#### 4.3.1 Introduction

This test method (E813-ASTM89) covers the determination of  $J_{IC}$  using fatigue cracked CT specimens. The property  $J_{IC}$  characterises the toughness of materials near the onset of crack extension from a pre-existing crack.

Testing involves an increasing tensile load being applied to a suitably precracked specimen. Measurements of applied load and load-line displacement are needed to obtain the total energy absorbed by the specimen. From this data a J-integral value is calculated and plotted against physical crack extension. This graph is then used to determine the  $J_{IC}$  value (Sections 4.3.3 and 4.3.4).  $J_{IC}$  can be converted to an equivalent stress intensity factor  $K_{Ic}$ . The conditions under which the test is conducted should then be considered when applying this  $K_{Ic}$  value to design. The evaluation of  $J_{IC}$  assumes slow-stable crack extension in a dominant linear elastic stress field.

In summary, this test method can serve the following purposes:

- establish a  $J_{IC}$  value which may be used as a ductile fracture toughness criterion to evaluate the effects of metallurgical variables, heat treatments and fabrication techniques;
- establish the suitability of a material for a specific application for which stress conditions are prescribed and flaw size limits are known with confidence; and
- establish a  $J_{IC}$  value for materials that lack sufficient thickness to be tested for  $K_{IC}$  (Section 4.2).

#### 4.3.2 Specimen size and apparatus

Testing apparatus required is identical to that described in Section 4.1.2. To reduce time and costs associated with all aspects of fracture testing, the CT specimens used in the determination of fatigue crack growth rates were used in this ductile fracture toughness testing. The two respective standards were used to ensure the precracking stage was such that the fracture toughness evaluation was valid.

Calibration of all measuring equipment is required prior to testing. The crack mouth opening displacement (clip) gauges should have an accuracy of 0.2 per cent over the working range and the load readings should have an accuracy of 1.0 per cent over the working range.

For a  $J_{IC}$  test to be considered valid, the following dimensions are required:

$$B \text{ and } b_0 \geq 25 \left( \frac{J_{IC}}{\sigma_{fs}} \right);$$

$$2 \leq \frac{W}{B} \leq 4 \text{ (} W = 2B \text{ is most common ratio used); and}$$

$$0.50 \leq \frac{a_0}{W} \leq 0.75 .$$

#### 4.3.3 Terminology and test procedure

See Section 4.1.3 for parameter definitions. The following list is a set of further definitions pertinent to this test method:

- J-integral,  $J$ , a mathematical expression, a line or surface integral that encloses the crack front from one crack surface to the other, used to characterise the local stress-strain field around the crack front;
- specimen thickness,  $B$ , distance between sides of specimen;
- net thickness,  $B_N$ , distance between the roots of the side grooves in side-grooved specimens,  $0.8 B$  is recommended for grooved specimens ;

- effective thickness,  $B_e$ , thickness term used in compliance-based calculations,  $B_e = B - (B - B_N)^2 / B$ ;
- physical crack size,  $a_p$ , distance from load-line to observed crack front;
- original crack size,  $a_o$ , physical crack size at the start of testing;
- original uncracked ligament,  $b_o$ , distance from the original crack front to the back surface of the specimen,  $b_o = W - a_o$  ;
- remaining ligament,  $b$ , distance from the physical crack front to the back surface of the specimen,  $b = W - a_p$  ;
- physical crack extension,  $\Delta a_p$ , increase in physical crack size,  $\Delta a_p = a_p - a_o$  ; and
- J-R curve, a plot of J-integral versus physical crack extension, J versus  $\Delta a_p$  .

The production of a satisfactory precrack is required before a valid  $J_{IC}$  test can commence. This precrack needs to extend past the notch by a minimum of 5 per cent of the crack size and not less than 1.3 mm. The precracking procedure used in this report consisted of the crack growth rate testing (Section 4.1). In addition to these guidelines, it is recommended that the final 0.64 mm of fatigue precrack be produced with a maximum load less than  $0.4P_L$ , (equation 4.9 calculates  $P_L$ ) or a load such that the ratio of applied stress intensity to the elastic modulus is less than  $0.0005 \text{ mm}^{1/2}$ . In order to produce acceptably straight precrack fronts, precracking should be completed with loads below  $P_L$  and before side-grooves are machined:

$$P_L = \frac{B b o^2 \sigma_{fs}}{2W + a} \quad (4.9)$$

The objective of this test method described below is to develop the initial portion of a J-R curve consisting of J-integral values at a series of measured specimen crack extensions from which an engineering estimate of the J-integral value can be estimated which corresponds to a small stable crack extension of 0.2 mm. It is considered good practice to test at least three specimens to ascertain the effects of material variability.

Upon completion of the precracking phase, the specimen is loaded in tension at a rate such that the time taken to reach a load of  $0.4 P_L$  is between 6 and 600 seconds. Both the applied load and load-line displacement are continuously recorded. These data are used to evaluate J from the area under the load-displacement record (Section 4.3.4) and for the elastic compliance method to infer crack length and hence crack extension. At regular intervals during the test, there should be unload / reload cycles. These cycles (compliance readings) are used to calculate the crack length. To evaluate enough suitable data points from the testing, a minimum of eight unload / reload cycles are recommended for the first 2.5 mm of crack extension. The suggested range for these unload / reload cycles should not exceed  $0.2 P_L$  or 50 per cent of the current load. The original crack length,  $a_o$ , should be measured at least three times using the compliance method before the loading is increased to cause initial crack extension. Calculated  $a_o$  values should not differ by more than 0.2 per cent of W from each other.

When a crack extension of approximately 2.5 mm is achieved, the load on the specimen should be removed. The next stage in testing is to mark the end of the crack extension for later evaluation. This can be done in one of two ways: remove the specimen and heat tint at about 300°C for 10 minutes; or fatigue cycle at 90 per cent of the final test load. The end of crack extension is marked by the end of the heat tint or the beginning of the second flat fatigue surface. The specimen should then be carefully broken to expose the crack surface. The front and rear of the stable crack extension should be visually measured at nine equally spaced points centred about the specimen centreline and extending to 0.005 W from the root of the side-grooves.  $a_o$  and  $a_p$  can then be calculated as follows: average the two surface values and combine with the remaining seven measurements to determine the average length.

#### 4.3.4 Interpretation of results

The precision of the  $J_{IC}$  determination depends on the errors in the load and displacement measurements. The variation in the areas under the load versus displacement curve used for J calculations resulting from the recommended measuring accuracy is 2 per cent. Likewise, the expected maximum error in crack growth extension is intended to be 15 per cent of the physical crack growth. The standard states there is no 'standard' value for  $J_{IC}$  for any material.

The first step in determining the  $J_{IC}$  value is to evaluate the J-integral and crack extension at each unload / reload stage in the applied load and loadline displacement data. For a compact specimen, the crack length is determined using the compliance method (equation 4.1) as restated below.

$$a = W (1.0002 - 4.0632 U_x + 11.242 U_x^2 - 106.04 U_x^3 + 464.33 U_x^4 - 650.68 U_x^5)$$

$$\text{where } U_x = \left\{ (EC_i B_e)^{1/2} + 1 \right\}^{-1};$$

E = effective modulus (to account for testing uncertainties, equation 4.10); and

$C_i$  = compliance = loadline displacement / applied load (for unload / reload sequence).

$$E = \frac{1}{C_o B_e} \left( \frac{W + a_o}{W - a_o} \right)^2 \left[ \begin{array}{l} 2.1630 + 12.219 \left( \frac{a_o}{W} \right) - 20.065 \left( \frac{a_o}{W} \right)^2 - 0.9925 \left( \frac{a_o}{W} \right)^3 \\ + 20.609 \left( \frac{a_o}{W} \right)^4 - 9.9314 \left( \frac{a_o}{W} \right)^5 \end{array} \right] \quad (4.10)$$

where  $C_o$  = initial specimen loadline compliance; and

$a_o$  = original crack size as physically measured.

The effective modulus, E, should be used to calculate all crack lengths for this specimen tested.

For a compact specimen, the J-integral is calculated according to equation 4.11.

$$J = J_e + J_p \quad (4.11)$$

where  $J_e$  = elastic component of J (equation 4.12); and  
 $J_p$  = plastic component of J (equation 4.13).

At a given point (i) corresponding to  $v_i$ ,  $P_i$  on the specimen load versus loadline displacement record:

$$J_{e(i)} = \frac{K_{(i)}^2(1-\nu^2)}{E} \quad (4.12)$$

where

$$K_{(i)} = \frac{P_i}{\sqrt{B B_N W}} \frac{\left(2 + \frac{a_o}{W}\right)}{\left(1 - \frac{a_o}{W}\right)^{3/2}} \left[ 0.886 + 4.64 \left(\frac{a_o}{W}\right) - 13.32 \left(\frac{a_o}{W}\right)^2 + 14.72 \left(\frac{a_o}{W}\right)^3 - 5.6 \left(\frac{a_o}{W}\right)^4 \right]$$

$$J_{p(i)} = \frac{\left(2 + \frac{0.522 b_o}{W}\right) A_{p(i)}}{B_N b_o} \quad (4.13)$$

where  $A_{p(i)}$  is the shaded area shown in Figure 4.7. This area can be calculated using numerical integration to an accuracy of no less than 2 per cent. The resulting value should be converted to the correct units (Joules).

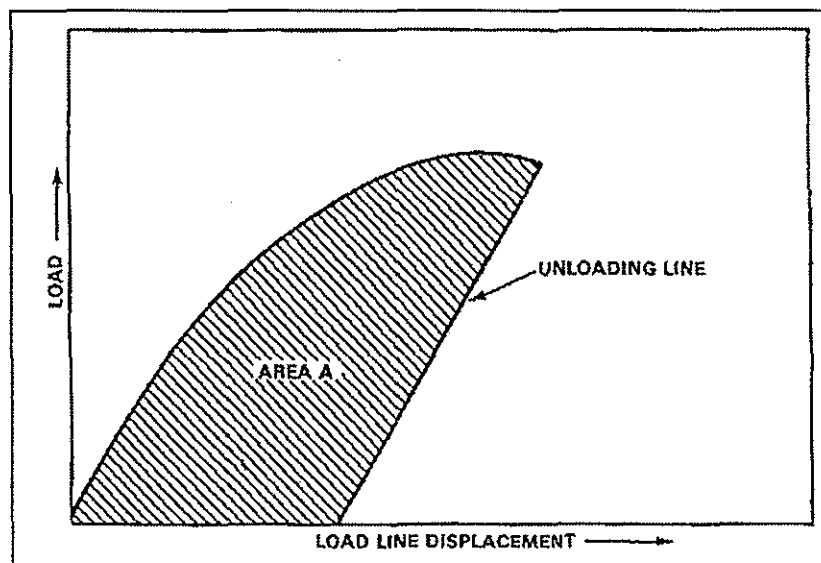


Figure 4.7 Definition of area used in J value calculation.

The total  $J$  value (converted into  $\text{kPa}\cdot\text{m}$ ) and the crack extension data points are plotted as shown in Figure 4.8.

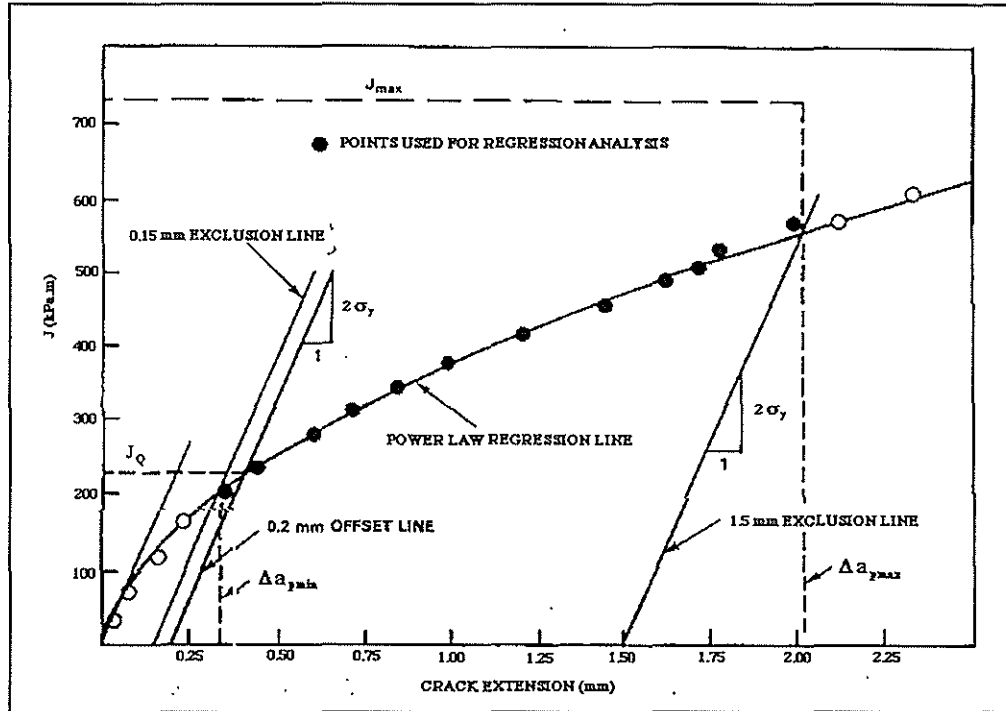


Figure 4.8: Definitions of data qualification (J-R plot).

As shown in Figure 4.8, a power law curve is fitted to qualified data points. Using a method of least squares, a linear regression line in the following form is determined:

$$\ln J = \ln C_1 + C_2 \ln (\Delta a_p) . \quad (4.14)$$

An iterative method is used to evaluate suitable (qualified) data points to be used in determining the power law curve. The process is started by calculating a best-fit power law curve from selected points deemed most appropriate. Figure 4.9 shows the region pertaining to valid data. As seen the valid data point region is bounded by five curves. The 0.15 mm and 1.5 mm 'exclusion' lines are produced by constructing curves with a slope equal to  $2\sigma_{fs}$  (or  $2\sigma_y$  as shown) which pass through the 0.15 mm and 1.5 mm points on the abscissa. The top bounding horizontal curve restricts  $J$  values to be below  $J_{\max}$  ( $= b_0\sigma_{fs}/15$ ). Vertical lines corresponding to  $\Delta a_{p \min}$  and  $\Delta a_{p \max}$  (values determined by the intersection of the exclusion lines and the first approximated power law curve) complete the region for bounding qualified data points. This process is repeated until no further data points are excluded or included in the qualifying region partly determined by updated power law curve. Four points should remain between  $\Delta a_{p \min}$  and  $\Delta a_{p \max}$ .